



ELSEVIER

Available online at www.sciencedirect.com

SCIENCE @ DIRECT®

Journal of Sound and Vibration 287 (2005) 865–882

JOURNAL OF
SOUND AND
VIBRATION

www.elsevier.com/locate/jsvi

Reliability-based critical earthquake load models. Part 1: linear structures

A.M. Abbas, C.S. Manohar*

Department of Civil Engineering, Indian Institute of Science, Bangalore 560012, India

Received 13 January 2004; received in revised form 6 September 2004; accepted 6 December 2004

Available online 16 February 2005

Abstract

In this two-parts study the problem of determining stochastic critical earthquake excitations for linear and nonlinear structural systems is considered. In the first part of the study attention is focussed on linear structures. The earthquake load is modelled as a partially specified Gaussian random process. The known information on the excitation involves bounds on total average energy, zero crossing rate and the amount of expected disorder quantified in terms of average entropy rate. The unknown power spectral density function of the earthquake acceleration is computed with three alternative objectives: (a) maximization of probability of exceedance of extreme value of the response over a given duration across a specified permissible limit, (b) minimization of the Hasofer–Lind reliability index associated with the performance criterion considered above and (c) maximization of the steady-state response variance. The relative scope of these methods is discussed. The optimal input power spectral density functions are shown to be nearly identical in all the three cases. The paper discusses the implications of this result and illustrates the formulations with reference to a steel frame and a stack-like structure.

© 2005 Elsevier Ltd. All rights reserved.

1. Introduction

Critical excitations are tailor-made to produce highest response in given engineering structures while, at the same time, they also satisfy a set of constraints that are reflective of known features

*Corresponding author. Tel.: +91 80 2293 3121; fax: +91 80 2360 0404.

E-mail addresses: amabbas@mail.com (A.M. Abbas), manohar@civil.iisc.ernet.in (C.S. Manohar).

of the excitations. In the context of earthquake engineering, the method of critical excitation offers an useful alternative in specifying earthquake load models for important engineering structures. The motivation for the development of these methods has been widely discussed in the existing literature: see, for example, the paper by Manohar and Sarkar [1] and the more recent comprehensive state of the art report by Takewaki [2]. Early work in this area of research has been due to Drenick [3], Shinozuka [4] and Iyengar [5]. These models can be developed within the frameworks of response spectra, time histories or random process modelling. Within the context of random critical earthquake excitation modelling, the idea of critical power spectral density (psd) functions that produce highest response variance for linear systems under constraints on total average energy has been studied by Iyengar and Manohar [6]. These authors modelled the ground acceleration as a nonstationary Gaussian random process obtained as a product of a known deterministic envelope function and an unknown zero mean Gaussian stationary random process. The unknown psd function was expanded as a linear combination in terms of orthonormal functions with undetermined coefficients. These coefficients were computed such that the response variance of a given system is maximized under a constraint on the input total average energy. In this paper, however, the frequency range of the critical input was not explicitly incorporated in the formulation. Iyengar [7] included the excitation frequency bandwidth into the formulation. Srinivasan et al. [8] modelled the earthquake acceleration as a nonstationary filtered shot noise and optimized the parameters of this model such that response of a given linear system is maximized. Manohar and Sarkar [1] introduced additional constraints on input zero crossing rate and also investigated the use of the entropy rate of the input in characterizing the amount of disorder to be expected in earthquake signals. As might be expected, with increases in entropy rate, the input signals tend to become rich in frequency content and, thus, these authors emphasized the effectiveness of entropy rate considerations in arriving at realistic critical earthquake load models.

Takewaki [9,10] has investigated the critical psd function models by introducing a new constraint on the peak of the input psd function in addition to that on the total average energy. This author has modelled the ground excitation as a stationary Gaussian random process and has optimized the structure response under these constraints [9]. Subsequently, Takewaki [10] generalized his earlier study to account for nonstationarity in the earthquake excitations. Khajehpour and Sarkar [11] and Sarkar and Khajehpour [12] model the critical acceleration as a stationary Gaussian random process with an unknown psd function which is computed such that the mean of the level crossing rate of response of a given linear structure as well as the input entropy rate are maximized under a constraint on the input variance. These authors have employed genetic algorithms based on Pareto optimization theory to solve this constrained nonlinear multi-objective optimization problem. Recently, the present authors accounted for the input entropy rate by treating it as an explicit constraint [13]. These authors estimated the information needed to impose the constraints on critical excitation by using past recorded earthquake accelerograms. The problem of formulating critical psd matrix models for multi-support and/or multi-component earthquake models has been studied by Sarkar and Manohar [14,15] and Abbas and Manohar [16].

In most of the studies reported above, the objective function in defining the critical excitation has been the variance of the response and the structural behavior has been assumed to be linear. Thus, these studies employ the well known input–output relations in time/frequency domains for

randomly driven systems. With a view to expand the capabilities of the method of critical excitations, it is clearly of interest to characterize system response in terms of reliability measures and, to take into account structural nonlinearities and multi-support nature of excitations. Also of interest is to treat structural parameters as being random in arriving at critical excitation–response pair. The present study, reported in two parts, is motivated by these considerations. Accordingly, in the first part of these studies, we begin by considering linear systems with the earthquake inputs modelled as zero mean Gaussian stationary random processes. The information available on the inputs is taken to include estimates of total average energy, average rate of zero crossings and the entropy rate. Three alternative objectives for finding critical responses are considered: these are, namely, (a) maximization of probability of exceedance of extreme value of the response over a given duration across a specified permissible limit, (b) minimization of the Hasofer–Lind reliability index associated with the performance criterion considered above and (c) maximization of the steady-state response variance. Illustrative examples on simple frame and stack-like structures demonstrate that all these three objective functions lead to similar critical input psd functions.

2. Method I: critical excitation that maximizes failure probability

2.1. Objective function

The equation of motion for the relative displacement $\mathbf{u}(t)$ of a discretized N -degree-of-freedom linear structure driven by a horizontal ground acceleration $\ddot{x}_g(t)$ at its base is well known to be given by

$$\mathbf{M}\ddot{\mathbf{u}}(t) + \mathbf{C}\dot{\mathbf{u}}(t) + \mathbf{K}\mathbf{u}(t) = -\mathbf{M}\{\mathbf{1}\}\ddot{x}_g(t). \quad (1)$$

Here \mathbf{M} , \mathbf{C} , \mathbf{K} , are, respectively, the mass, damping and stiffness matrices of the discretized structure, and $\{\mathbf{1}\}$ represents a column vector of ones. In the present study, the damping is taken to be proportional, and, also, it is assumed that system starts from rest. The structural matrices here are taken to be deterministic in nature. As is well known, for these systems, any response quantity such as a displacement, or a linear transformation of displacement, such as, stress component or stress resultant, is also a Gaussian random process. We denote this response quantity by $L(t)$ and, following standard terminology used in structural reliability, we designate it by the term ‘load effect’. Associated with the load effect, $L(t)$, there exists an associated structural capacity and this is denoted by R . Thus, for example, $L(t)$ = displacement component at a specified point on the structure and R = permissible displacement at this point; similarly, $L(t)$ = maximum bending moment or shear force at the base and R = moment or shear capacity of the structure at the same point. Let $1 - P_f$ = the probability that the load effect remains less than the load-carrying capacity over the time interval $(0, T_d)$. That is,

$$1 - P_f = P[R - |L(t)| > 0; \forall t \in (0, T_d)]. \quad (2)$$

Here P_f is the probability of structural failure. The determination of P_f , as given by the above equation, constitutes a problem in time-variant reliability analysis. Introducing the random variable $L_m = \max_{0 < t < T_d} |L(t)|$, the failure probability can also be expressed in a time-invariant

format as

$$P_f = P[R - L_m < 0] = \underbrace{\int \int}_{r-l < 0} p_{RL_m}(r, l) dr dl. \tag{3}$$

Here $p_{RL_m}(r, l)$ is the joint probability density function of R and L_m and, to proceed further, a suitable model for this quantity is needed. It is of interest to note that the potential sources of uncertainties here are in the specification of loads and structural properties (such as stiffness, mass, damping and strength characteristics). The uncertainties in ground acceleration arise due to uncertainties in source mechanism, quantum of energy released, location of energy source, geological medium through which the waves travel, and local soil conditions. On the other hand, structural uncertainties could arise due to intrinsic material variabilities, and uncertainties in details of soil structure interactions, manufacture of the construction material and details of actual construction. Thus, at the outset, it appears reasonable to assume that the earthquake loads and the random variables that model structural uncertainties (such as stiffness, mass, damping and load-carrying capacity) could be treated as being stochastically independent. However, it might be argued that, in any design problem, since the structural capacities are indeed provided to meet the imposed demands of the load effects, these two quantities (namely, structural capacity and load effect) are going to be mutually dependent. The main difficulty, in our opinion, here lies not so much in capabilities of the underlying mathematical model to handle such dependencies, but more so in being able to quantify the measures of such dependencies. Therefore, in the development of the present method, we proceed with the assumption that the load effect and the capacity are taken to be stochastically independent. Also, in evaluating the load effects we assume here that the structural stiffness, mass and damping properties are deterministic in nature. A more general method, that avoids some of these assumptions, is being presented in the next section.

Under the assumptions stated above, it can be shown that Eq. (3) can be simplified to get

$$P_f = \int_0^\infty P_R(l)p_{L_m}(l) dl, \tag{4}$$

where $P_R(r)$ is the probability distribution function of R , and $p_{L_m}(l)$ is the probability density function (pdf) of L_m . Based on the theory of extreme values of stationary Gaussian random processes [17], the probability distribution of L_m , after $L(t)$ has reached a steady state, can be approximated by

$$P_{L_m}(l) = \exp\left[-N_0^+ T_d \exp\left(-\frac{l^2}{2\sigma_{0L}^2}\right)\right], \quad 0 \leq l \leq \infty. \tag{5}$$

Here N_0^+ is the average rate of zero crossing of the response process $L(t)$ given by $N_0^+ = (1/(2\pi))\sqrt{\sigma_{2L}^2/\sigma_{0L}^2}$, in which, σ_{0L}^2 and σ_{2L}^2 are, respectively, the zeroth and the second spectral moments of the process $L(t)$. These quantities, in turn, are given in terms of the psd function, $S(\omega)$, of the input acceleration $\ddot{x}_g(t)$ as

$$\sigma_{0L}^2 = \int_{\omega_0}^{\omega_c} |H_L(\omega)|^2 S(\omega) d\omega, \quad \sigma_{2L}^2 = \int_{\omega_0}^{\omega_c} \omega^2 |H_L(\omega)|^2 S(\omega) d\omega. \tag{6}$$

In these expressions, $H_L(\omega)$ is the frequency response function associated with the response quantity $L(t)$ and (ω_0, ω_c) is the frequency bandwidth of the ground acceleration $\ddot{x}_g(t)$.

2.2. Constraints

The problem of modelling critical excitations can now be stated as finding $S(\omega)$ which maximizes P_f as given by Eq. (4), subject to a set of suitable constraints. A measure of total average energy, given by,

$$E_0 = \int_{\omega_0}^{\omega_c} S(\omega) d\omega \tag{7}$$

is helpful in defining the size of the earthquake. The imposition of this constraint alone would lead to overly conservative estimates of the highest response [1]. This has been mainly due to the highly resonant characteristics of the resulting critical excitations. In other words, the frequency content of the critical excitations, in these cases, turns out to be unrealistic when compared to the frequency content of recorded earthquake accelerograms. Within the framework of method of critical excitations, any characteristic of a future earthquake, which one can anticipate with confidence, needs to be incorporated into the modelling exercise through appropriate constraints. Therefore, the question arises on the nature of constraints that help us to quantify the frequency content that the critical excitation should possess. Imposition of such a constraint is an essential requirement in the development of a useful critical excitation model. In our earlier studies we have considered this question and have explored imposing the following constraints:

- average rate of zero crossing [1,13] given by

$$n_0^+ = 1/(2\pi)\sqrt{(E_2/E_0)}, \quad E_2 = \int_{\omega_0}^{\omega_c} \omega^2 S(\omega) d\omega \tag{8}$$

- an upper bound and a lower bound on the Fourier amplitude spectrum of the ground acceleration [13], and/or
- average rate of entropy of the acceleration process [1,13,15].

The study by Manohar and Sarkar [1] has shown the ineffectiveness of constraint on average rate of zero crossings in imparting realistic frequency content to the critical excitations. The second option, namely, the bounds on Fourier amplitude spectra, works successfully within deterministic framework but places serious demands on our ability to specify these constraints [13]. Within the framework of random process models for critical excitations, we have found that a constraint on average entropy rate to be worthy of serious consideration. In this context, it may be recalled that, for a zero mean, band limited, stationary Gaussian random process $\xi(t)$ with psd function $S(\omega)$, the average entropy rate is given by [1]

$$\bar{H} = \log_e \sqrt{2\pi e} + \frac{1}{2(\omega_c - \omega_0)} \int_{\omega_0}^{\omega_c} \log_e S(\omega) d\omega. \tag{9}$$

Here (ω_0, ω_c) is the frequency bandwidth. Let us consider two alternative models for $\zeta(t)$: one that is narrow banded and the other broad banded. Let us assume that these two processes have the same variances. The time realization of a narrow band process would be fairly ‘ordered’ and its spectrum highly localized in frequency. Conversely, the time realization of a band-limited white noise would be relatively more ‘disordered’ and the spectrum would be wide spread or the signal rich in frequency content. If one computes the entropy rate for these two processes, it turns out that the entropy rate of the wide band signal would be higher than that of the narrow band process. The proposition in our studies has been that this relationship between entropy rate, frequency content and disorder can be used in specifying the frequency content that one can expect in the critical earthquake excitation. It may also be noted in this context that entropy-based principles offer powerful modelling tools in the treatment of random phenomena with incompletely specified probability space. Given the fact that the random critical excitation models essentially deal with incompletely specified random processes, it is reasonable to expect that the concept of entropy rate has bearing on the development of these models. In the computational work it has been found advantageous to express the average entropy rate of $\zeta(t)$ in terms of the increase in the average entropy rate when $\zeta(t)$ is added to a reference band-limited white noise process of intensity S_0 . It can be shown that this increase is given by

$$\Delta\bar{H} = \frac{1}{2(\omega_c - \omega_0)} \int_{\omega_0}^{\omega_c} \log_e \left[1.0 + \frac{S(\omega)}{S_0} \right] d\omega. \quad (10)$$

This representation can be thought of as being akin to the decibel scales often used in describing frequency response functions and other spectral quantities in vibration engineering where in quantities of interest are expressed relative to an arbitrarily established reference value. The main advantage in adopting this definition, in the context of critical excitation modelling, has been that computational problems in evaluating \bar{H} when $S(\omega)$ becomes small for any value of ω in $[\omega_0, \omega_c]$ can be avoided. Thus, in the present study the critical excitations are taken to satisfy the constraint

$$\frac{1}{2(\omega_c - \omega_0)} \int_{\omega_0}^{\omega_c} \log_e \left[1.0 + \frac{S(\omega)}{S_0} \right] d\omega \geq \Delta\bar{H}_W. \quad (11)$$

Here $\Delta\bar{H}_W$ is the estimate of $\Delta\bar{H}$ that one can expect in realistic earthquake records. The problem of estimating $\Delta\bar{H}_W$ has been addressed in one of our earlier studies [13].

2.3. Solution procedure

The problem of determining the critical excitation model can now be stated as finding $S(\omega)$ which maximizes P_f (4) under the constraints given by Eqs. (7,8) and (11). Clearly, this problem constitutes a constrained nonlinear optimization problem. To solve this problem, we first represent $\ddot{x}_g(t)$ in a random harmonic series as $\ddot{x}_g(t) = \sum_{n=1}^{N_f} \{A_n \cos \Omega_n t + B_n \sin \Omega_n t\}$. Here, $\{A_n, B_n\}_{n=1}^{N_f}$ is a set of $2N_f$ zero mean Gaussian random variables and N_f is the number of discrete frequencies included in the series representation for $\ddot{x}_g(t)$ within (ω_0, ω_c) . Furthermore, the random variables A_n and B_n are taken to be such that $\langle A_n A_m \rangle = \sigma_n^2 \delta_{mn}$, $\langle B_n B_m \rangle = \sigma_n^2 \delta_{mn}$ and $\langle A_n B_m \rangle = 0 \forall n, m = 1, 2, \dots, N_f$. Here $\langle \cdot \rangle$ represents the mathematical expectation operator and δ_{mn} is the Kronecker delta. These conditions ensure that $\ddot{x}_g(t)$ is a wide sense stationary random

process. This representation also automatically discretizes $S(\omega)$ in terms of the deterministic quantities, σ_n^2 , and is given by $S(\omega) = \sum_{n=1}^{N_f} \sigma_n^2 \delta(\omega - \Omega_n)$ where, $\delta(\cdot)$ represents the Dirac delta function. Consequently, the optimization problem defined above can be restated in a discrete form as finding $\{\sigma_n^2\}_{n=1}^{N_f}$ which maximize P_f , as given by Eq. (4), with

$$p_{L_m}(l) = \frac{N_0^+ T_d l}{\sigma_{0L}^2} \exp \left[-\frac{l^2 + 2N_0^+ T_d \sigma_{0L}^2 \exp(-l^2/(2\sigma_{0L}^2))}{2\sigma_{0L}^2} \right],$$

$$N_0^+ = \frac{\frac{1}{2\pi} \sqrt{\sum_{n=1}^{N_f} \Omega_n^2 |H_L(\Omega_n)|^2 \sigma_n^2 / \sum_{n=1}^{N_f} |H_L(\Omega_n)|^2 \sigma_n^2}}{\sum_{n=1}^{N_f} |H_L(\Omega_n)|^2 \sigma_n^2}, \quad \sigma_{0L}^2 = \sum_{n=1}^{N_f} |H_L(\Omega_n)|^2 \sigma_n^2, \quad (12)$$

subject to the constraints

$$\sum_{n=1}^{N_f} \sigma_n^2 = E_0, \quad \sum_{n=1}^{N_f} \sigma_n^2 \Omega_n^2 = E_2, \quad \sigma_n^2 \geq 0,$$

$$\frac{1}{2(\omega_c - \omega_0)} \sum_{n=1}^{N_f} (\Omega_n - \Omega_{n-1}) \log_e \left[1.0 + \frac{\sigma_n^2}{S_0(\Omega_n - \Omega_{n-1})} \right] \geq \Delta \tilde{H}_W. \quad (13)$$

Thus it follows that the objective function, as given by Eq. (12), as well as the constraints listed above are nonlinear functions of the optimization variables $\{\sigma_n^2\}_{n=1}^{N_f}$, and, therefore, the problem of finding critical excitation here constitutes a nonlinear optimization problem. It is proposed in the present study to solve this problem by using the sequential quadratic programming method as available in the Matlab optimization toolbox [18]. This leads to an iterative procedure to determine the optimal solution with the attendant need for specifying an appropriate starting solution. At every i th step of iteration, the convergence criteria $|P_{f_i} - P_{f_{i-1}}| \leq \ell_1$ and $|\sigma_{n_i}^2 - \sigma_{n_{i-1}}^2| \leq \ell_2$ are checked and the process terminates if these conditions are met.

3. Method II: critical excitation that minimizes reliability index

The problem of determination of the failure probability by the evaluation of the double integral appearing in Eq. (3) can be side-stepped if attention is shifted to the determination of an associated reliability index. The theory of reliability indices is well developed and is discussed extensively in the literature, see, for example, the text book by Ang and Tang [19]. One of the commonly used reliability index is the Hasofer–Lind reliability index which is defined as the shortest distance from the origin to the limit surface in the space of standard normal random variables [20]. A basic property of reliability indices is that an increase in their value is expected to imply a reduction in the failure probability. In the context of critical earthquake excitations, one can now introduce a new definition for the critical excitation as the excitation that minimizes the reliability index associated with the performance function $g(R, L_m) = R - L_m$ under a set of specified constraints. The basic motivation for introducing this definition is the expectation that this definition is more generally applicable than the definition proposed in the previous section.

This point would be elaborated upon during the later part of this paper and in the next part of this paper [21].

To formulate the problem of deriving critical seismic loads as per the new definition proposed above, we first note that the structure performance function is given in terms of two random variables, namely, the structure capacity, R , and the load effect, L_m , as

$$g(\mathbf{X}) = R - \max_{0 < t < T_d} |L(t)| = R - L_m. \quad (14)$$

Here $\mathbf{X} = [R \ L_m]^t = [X_1 \ X_2]^t$ is the vector of the two random variables, R and L_m . In case, the mass, stiffness and damping characteristics are also modelled as being random, the definition of X can be extended to include these random variables also. Furthermore, the elements of X , in general, can be modelled as being jointly non-Gaussian and mutually dependent. For the purpose of illustration, we restrict our attention here to the case when X consists of only two random variables, namely, R and L_m . It is to be noted that $g(\mathbf{X}) > 0$ defines the safe region, $g(\mathbf{X}) < 0$ indicates the failure region and $g(\mathbf{X}) = 0$ defines the failure surface. The above performance function is linear in two non-Gaussian random variables. The problem of determining the reliability index for such performance functions is well studied in the literature (see, for example, Ref. [19]). Here one begins by transforming the vector of random variables \mathbf{X} to a vector of uncorrelated Gaussian random variables denoted by $\mathbf{X}^N = [X_1^N \ X_2^N]^t$ using the conditions

$$\Phi\left(\frac{x_i^* - \mu_{X_i}^N}{\sigma_{X_i}^N}\right) = P_{X_i}(x_i^*), \quad \frac{1}{\sigma_{X_i}^N} \phi\left(\frac{x_i^* - \mu_{X_i}^N}{\sigma_{X_i}^N}\right) = p_{X_i}(x_i^*). \quad (15)$$

Here x_i^* ($i = 1, 2$) is the design point, that is, the point on the limit surface with the smallest Euclidean norm in the standard normal space, $P_{X_i}(\cdot)$, $p_{X_i}(\cdot)$, are respectively, the probability distribution and density functions of the original random variables X_i ($i = 1, 2$), $\Phi(\cdot)$, $\phi(\cdot)$, are the standard normal probability distribution and density functions, respectively, and $\mu_{X_i}^N$, $\sigma_{X_i}^N$ are the mean and standard deviation of the equivalent normal variate. Following Ang and Tang [19], it can be shown that $\mu_{X_i}^N$ and $\sigma_{X_i}^N$ are given, respectively, by

$$\sigma_{X_i}^N = \frac{\phi\{\Phi^{-1}[P_{X_i}(x_i^*)]\}}{p_{X_i}(x_i^*)}, \quad \mu_{X_i}^N = x_i^* - \sigma_{X_i}^N \Phi^{-1}[P_{X_i}(x_i^*)]. \quad (16)$$

Accordingly, the structural safety can now be measured in terms of the Hasofer–Lind reliability index, β_{HL} , as the shortest distance from the origin to the failure surface in the equivalent standard normal space, \mathbf{X}^N [20]. It follows from Eq. (14) that β_{HL} is given by

$$\beta_{HL} = \frac{\mu_{X_1}^N - \mu_{X_2}^N}{\sqrt{(\sigma_{X_1}^N)^2 + (\sigma_{X_2}^N)^2}}. \quad (17)$$

Furthermore, the failure point in the original space is given by

$$x_i^* = \sigma_{X_1}^N x_i^{N*} + \mu_{X_2}^N = -\alpha_i \beta_{HL} \sigma_{X_1}^N + \mu_{X_2}^N, \quad \alpha_i = \frac{\partial g / \partial X_i^N |_{x_i^*}}{\sqrt{\sum_{i=1}^2 (\partial g / \partial X_i^N |_{x_i^*})^2}}, \quad i = 1, 2. \quad (18)$$

Here α_i is the vector of the direction cosines associated with the check point. To formulate the problem of deriving critical earthquake excitations, the ground motion $\ddot{x}_g(t)$ is again expanded in a Fourier series as has been done in the previous section. Thus, the problem of finding critical excitation can now be stated as computing the optimal $\{\sigma_n^2\}_{n=1}^{N_f}$ that minimize the structural reliability index

$$\beta_{HL} = \frac{x_1^* - x_2^* - \sigma_{X_1}^N \Phi^{-1}[P_{X_1}(x_1^*)] + \sigma_{X_2}^N \Phi^{-1}[P_{X_2}(x_2^*)]}{\sqrt{[\phi\{\Phi^{-1}[P_{X_1}(x_1^*)]\}/p_{X_1}(x_1^*)]^2 + [\phi\{\Phi^{-1}[P_{X_2}(x_2^*)]\}/p_{X_2}(x_2^*)]^2}} \quad (19)$$

subject to the constraints listed in Eq. (13). It is to be noted that the right-hand side of the above equation is implicitly dependent upon the optimization variables, $\{\sigma_n^2\}_{n=1}^{N_f}$ in a nonlinear manner. Thus the optimization problem here again constitutes a constrained nonlinear optimization problem. The solution to this problem is obtained using the sequential quadratic programming method as has been done earlier in the previous section. Here again an iterative procedure is required for the solution in which, within each step, the Hasofer–Lind reliability index is estimated. At every step of iteration, the convergence criteria $|\beta_{HL_i} - \beta_{HL_{i-1}}| < \delta_1$, $|g_i(\mathbf{x}^*)| < \delta_2$ and $|\sigma_{n_i}^2 - \sigma_{n_{i-1}}^2| < \ell_2$ are checked and the process terminates if these conditions are met.

4. Method III: critical excitation that maximizes response variance

Here the critical psd function is determined such that the response variance in the steady state is given by

$$\sigma_{0L}^2 = \int_{\omega_0}^{\omega_c} |H_L(\omega)|^2 S(\omega) d\omega \quad (20)$$

is maximized subject to the constraints listed in Eq. (13). This model of critical excitations has been recently studied by the present authors [13] and the details are omitted here. The results from this model are included in the present study to enable a comparison between the alternative critical input psd function models.

5. Numerical results and discussions on methods I, II and III

Two example structures are considered for illustrating the critical excitation models formulated in the preceding sections (Fig. 1). The first structure is a one-story portal frame and the second is a tall reinforced concrete chimney. The two structures are assumed to be located at a firm soil site and are subjected to a horizontal component of the ground motion. Table 1 summarizes the objective function, as well as the combination of constraints scenarios considered in the numerical illustrations. A set of ten horizontal ground motion is used in quantifying the constraints that are relevant in deriving the critical earthquake excitations. The details of the recorded accelerograms included in these calculations are summarized in Ref. [13] and these details are not repeated here. In the numerical calculations it is assumed that $E_0 = 1.45 \text{ m}^2/\text{s}^4$ and $n_0^+ = 1.64/\text{s}$. This leads to $E_2 = 153.96 \text{ m}^2/\text{s}^6$, which implies that the expected peak value of $\ddot{x}_g(t)$ is about $0.44g$. The

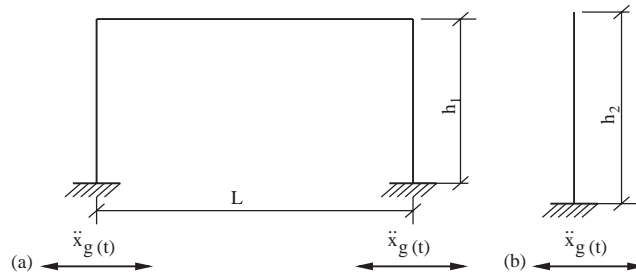


Fig. 1. Example structures considered. (a) Frame structure, (b) chimney.

Table 1
Nomenclature of objective function and combinations of constraints

Method	Objective	Constraints imposed	
		Case 1	Case 2
I	To maximize P_f	E_0 & n_0^+	E_0, n_0^+ & $\Delta\bar{H}_W$
II	To minimize β_{HL}	E_0 & n_0^+	E_0, n_0^+ & $\Delta\bar{H}_W$
III	To maximize σ_{uk}^2	E_0 & n_0^+	E_0, n_0^+ & $\Delta\bar{H}_W$

frequency bandwidth, (ω_0, ω_c) is taken as $(0, 25.00)$ Hz and the increase of average entropy rate, $\Delta\bar{H}_W$, from a reference white noise of intensity parameter $S_0 = 0.02 \text{ m}^2/\text{s}^3$, was computed to be 0.63. The total duration of the critical earthquake signal is taken as $T_d = 30$ s. The convergence parameters for method I are taken as $\ell_1 = 10^{-8}$ and $\ell_2 = 10^{-6}$, while those for method II are $\delta_1 = \delta_2 = 0.001$.

5.1. Example 1: seismic response of a steel frame

A one-story steel portal frame of width $L = 9.14$ m, height $h_1 = 5.49$ m and modulus of elasticity $E = 2.10 \times 10^{11} \text{ N/m}^2$ is considered, see Fig. 1(a). The frame carries a total dead load of $3 \times 10^3 \text{ N/m}$, and the columns are made of $W10 \times 33$ of A36 steel grade [22]. For purpose of dynamic analysis, it is assumed that the girder is sufficiently rigid to prevent rotation and that the columns are massless. Under these conditions, a single-degree-of-freedom (sdf) system is used to model the frame structure. The natural frequency of the frame is computed to be 2.07 Hz. A modal viscous damping of 3% is assumed. The number of frequency terms, N_f , in the series representation of $S(\omega)$, is taken to be 41. For the present sdf system, the frequency response function, $H(\omega)$, is given by $H_L(\omega) = 1/[\omega_n^2 - \omega^2 + 2j\zeta_n\omega_n\omega]$, where, ω_n and ζ_n are the natural frequency and damping ratio of the structure and $j = \sqrt{-1}$. Referring to Eqs. (1) and (14), and considering the force in the spring to be the criterion for failure, the performance function can be written as $g(\mathbf{X}) = R - k \max_{0 < t < T_d} |u(t)| = R - L_m$. Here, R , the resistance is a random variable and is taken as the maximum permissible force (yield force) in the spring. In the present work, two

different distributions, namely, normal distribution and type I asymptotic distribution are assumed for R . Furthermore, the mean and standard deviation of R are taken to be $\mu_R = 3.75 \times 10^4$ N, and $\sigma_R = 3.75 \times 10^3$ N for both the two distributions. It is to be noted that, the assumed value for μ_R implies that the allowable average yield stress in the spring is around 360 N/mm². The probability distribution function of the resistance when R is taken to be normal, is given by

$$P_R(r) = \frac{1}{2} \left\{ 1 + \operatorname{erf} \left(\frac{r - \mu_R}{\sqrt{2}\sigma_R} \right) \right\} \tag{21}$$

similarly, when R is type I asymptotic, one gets

$$P_R(r) = \exp[-\exp\{-\alpha(r - \varrho)\}], \quad \alpha = \frac{\pi}{\sqrt{6}\mu_R}, \quad \varrho = \mu_R - \frac{0.5770}{\alpha}. \tag{22}$$

The stiffness of the spring, k , was computed to be 4.67×10^5 N/m. In the performance function as defined above, L_m is a random variable, representing the maximum value of the response process $ku(t)$ over the time interval T_d after $u(t)$ has reached a stochastic steady state. Under the assumption that, $\ddot{x}_g(t)$ is a stationary Gaussian random process, the displacement response $u(t)$ is a stationary narrow band Gaussian random process. Therefore, the extreme value distribution of the response process, $u(t)$, that is $P_{U_m}(u_m)$, can be taken to be given by [17]

$$P_{U_m}(u_m) = \exp \left[-N_0^+ T_d \exp \left(-\frac{u_m^2}{2\sigma_{0L}^2} \right) \right]. \tag{23}$$

Consequently, the probability density function, $p_{U_m}(u_m)$ is now deduced as follows:

$$p_{U_m}(u_m) = \frac{N_0^+ T_d u_m}{\sigma_{0L}^2} \exp \left[-\frac{u_m^2 + 2N_0^+ T_d \sigma_{0L}^2 \exp(-u_m^2/(2\sigma_{0L}^2))}{2\sigma_{0L}^2} \right]. \tag{24}$$

Using transformation of random variables, the pdf of L_m can be shown to be given by

$$p_{L_m}(l) = \frac{N_0^+ T_d l}{k^2 \sigma_{0L}^2} \exp \left[-\frac{(l^2/k^2) + 2N_0^+ T_d \sigma_{0L}^2 \exp(-l^2/(2k^2 \sigma_{0L}^2))}{2\sigma_{0L}^2} \right]. \tag{25}$$

Fig. 2 shows the plots of critical input psd functions for the three models and two constraint scenarios listed in Table 1. Table 2 provides the results on the critical responses obtained using these models. This table also shows two additional sets of results, namely, (a) results on critical responses when the frame is re-designed to possess a higher natural frequency of 2.94 Hz, and (b) structure responses for $\omega_n = 2.07$ and 2.94 Hz when the system is driven by stationary random process with Kanai–Tajimi psd function. It is to be noted that the change in natural frequency of the system from an initial value of 2.07 Hz to a higher value of 2.94 Hz was realized by changing the mass of the frame keeping stiffness properties unaltered. Also, the Kanai–Tajimi psd function used herein is selected to be valid for a firm ground with variance equal to that of the critical psd functions. For the purpose of illustration, the plots of critical failure probability obtained using method I and the critical reliability index obtained using method II are shown in Fig. 3 for different values of μ_R keeping the distribution of R to be the type I extreme value. To investigate the effect of changing the constraint parameters on the critical inputs, a numerical investigation of the sensitivity of the critical response with respect to the constraint parameters is carried out. With

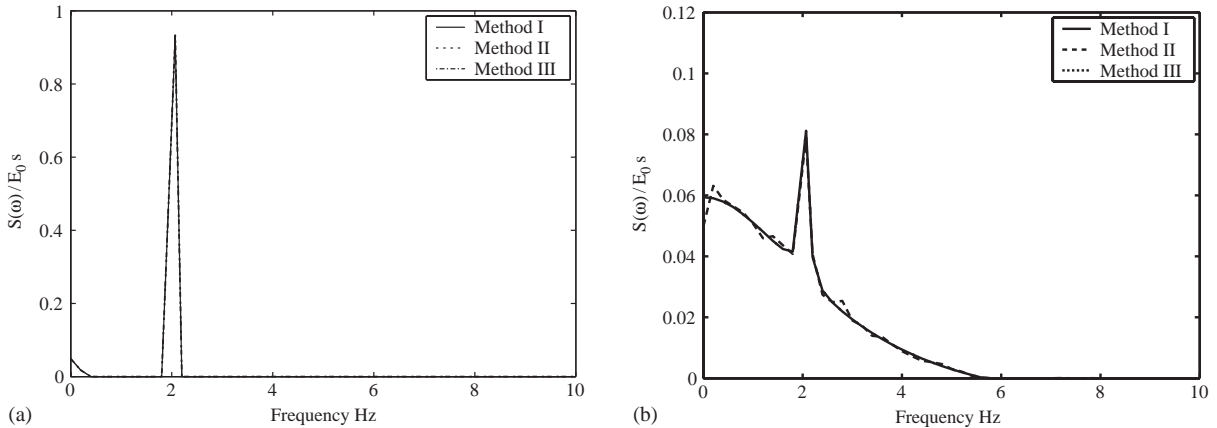


Fig. 2. Example 1: psd of $\ddot{x}_g(t)$. (a) Case 1, (b) case 2, $\omega_n = 2.07$ Hz, $\zeta_n = 0.03$, $\mu_R = 3.75 \times 10^4$ N, R is normal.

Table 2

Summary of P_f and β_{HL} for the steel frame, $\mu_R = 3.75 \times 10^4$ N, R is normal

Input	Critical psd				Kanai–Tajimi psd	
	$\omega_n = 2.07$ Hz, $\zeta_n = 0.03$		$\omega_n = 2.94$ Hz, $\zeta_n = 0.03$		$\omega_n = 2.07$ Hz	$\omega_n = 2.94$ Hz
	Case 1	Case 2	Case 1	Case 2	$\zeta_n = 0.03$	$\zeta_n = 0.03$
P_f	0.9997	0.0936	0.1485	1.12×10^{-4}	0.0390	6.45×10^{-5}
β_{HL}	-0.2602	0.2397	0.0976	1.6304	—	—
$\sigma_u(m)$	0.0607	0.0268	0.0226	0.0129	0.0197	0.0105

a change of 1% in each constraint parameters E_0 , n_0^+ , and $\Delta \bar{H}_W$, while other constraint parameters are kept unchanged, the values of P_f are computed by re-solving the optimization problem. The percentage changes in P_f due to changes of 1% in these parameters were computed to be 1.65, 0.56 and 4.32, respectively. This shows that the structure failure probability is more sensitive to the entropy rate constraint as compared with the energy and the zero crossing rate constraints. Based on the study of the numerical results, the following observations are made:

- (1) It is observed that all the three methods (I, II and III) lead to nearly the same critical psd function (Fig. 2(a) and (b)) for the two constraints scenarios (see Table 1). Given that the objective functions in these three cases are nonlinearly dependent on variables of optimization in significantly different manner, it is not obvious at the outset that these three methods must lead to the same critical psd function. However, from a physical perspective, of course, the result does not come as a surprise. The definition of critical inputs as per method III does not take into account randomness in resistance variables. It is of interest to note that the critical input psd function here, also, is similar to those obtained in methods I and II. This leads to the

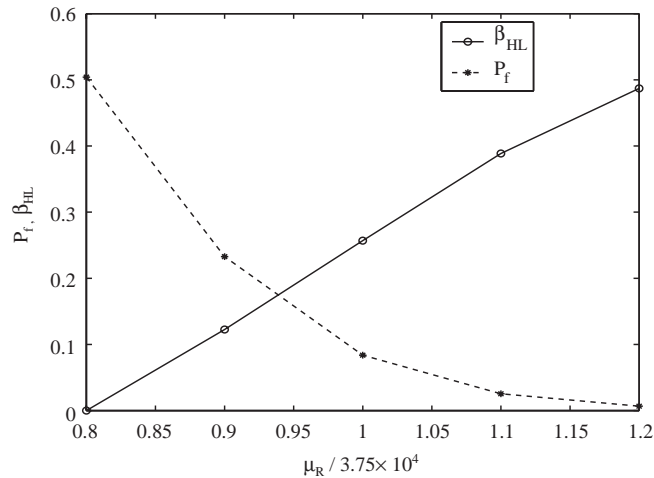


Fig. 3. Example 1: critical P_f obtained using method I and critical β_{HL} obtained using method II, for alternative values of μ_R for case 2; R is type I asymptotic.

conclusion that, for the example structure studied, randomness in resistance R does not influence the critical input significantly. The critical responses (in methods I and II), however, are found to be strongly influenced by models adopted for R .

- (2) When the constraints imposed include E_0 and n_0^+ (case 1), the critical psd function is highly resonant in nature with most of the energy located at the system natural frequency and a minor part located at $\omega = \omega_0$ (Fig. 2(a)). The occurrence of this secondary peak enables the satisfaction of the constraint on zero crossing rate. Consequently, it can be expected that the structure probability of failure tends to become high and, conversely, the reliability index becomes very low. Indeed, from Table 2, it can be seen that P_f and β_{HL} are, respectively, 0.9997 and -0.2602 (see column 2 of the table). The system natural frequency in this case is 2.07 Hz and the input zero crossing rate is 1.64/s. If a system with a natural frequency of 2.94 Hz is selected, the difference between the input zero crossing rate and the system natural frequency further increases and this is seen to lower the critical failure probability and increase the reliability index (see column 4 of Table 2).
- (3) With the introduction of the constraint on entropy rate (case 2), see Fig. 2(b), as might be expected, the critical input becomes relatively broad banded. More importantly, the psd function of the critical ground acceleration from all the three methods are seen to be nearly identical. The failure probability in this case drops significantly which can be seen from Table 2 (columns 3 and 5).
- (4) The orderability relationship that exists between the critical structure probability of failure obtained using method I and the critical reliability index obtained using method II, can be evidenced from Fig. 3, where a drop in the failure probability, with changes in μ_R , is always associated with an increase in the associated reliability index.
- (5) From Table 2 it can be observed that the ratio of P_f produced by critical inputs (case 2) to that from ground motion that has the Kanai–Tajimi psd function, that is valid for a firm soil site, and, has the same input energy, is around 2.40 and 1.74 for $\omega_n = 2.07$ and 2.94 Hz,

respectively. Similarly, the ratios on response standard deviation from method III are seen to be 1.36 and 1.23, respectively. These ratios provide an idea on the level of conservatism associated with critical excitation models.

5.2. Example 2: seismic response of a chimney

To illustrate the formulations developed in this study for multi-degree-of-freedom systems, a 46 m tall reinforced concrete chimney is considered, see Fig. 1(b). The chimney is taken to have uniform circular cross-section of 3.80 m outer diameter, 3.30 m inner diameter, constant mass density of 2500 kg/m^3 and modulus of elasticity $E = 2.0 \times 10^{10} \text{ N/m}^2$. A finite element analysis using 20 two-noded beam elements showed that the first four natural frequencies of the chimney are 0.94, 5.90, 16.52 and 32.36 Hz. Since the frequency bandwidth (ω_0, ω_c) of the input acceleration is taken to be (0, 25.00) Hz, the first three natural frequencies of the chimney are only retained in the dynamic analysis. The number of frequency terms, N_f , in the series representation is taken to be 31 and a modal viscous damping of 5% is assumed for the three modes. The resistance, R , is defined as the maximum allowable tip relative displacement that the chimney can sustain without failure and is taken as a deterministic quantity, $R = h_2/75 = 0.6133 \text{ m}$. The load effect, L_m , is taken as $\max_{0 < t < T_d} |u(t)|$ with probability distribution function, $P_{L_m}(l)$ given by Eq. (5). Critical earthquake excitations are computed using methods I and III. Fig. 4 shows the critical input psd function obtained using methods I and III for the constraint scenarios of cases 1 and 2 (see Table 1). As has been observed in the previous example, the two critical psd function models are seen to be identical in this case also. It is also observed that the response is dominated by the first mode contributions. The structure probability of failure under the action of critical inputs reduces from a value of 0.9999 to 0.1107 as the constraint on entropy rate is brought in. This is reflected in Fig. 5, in which, the pdf of L_m is shown for the two cases of constraints scenarios considered. Similarly, the effect of introducing the entropy rate constraint in method III was also observed to reduce the critical response standard deviation of the tip relative

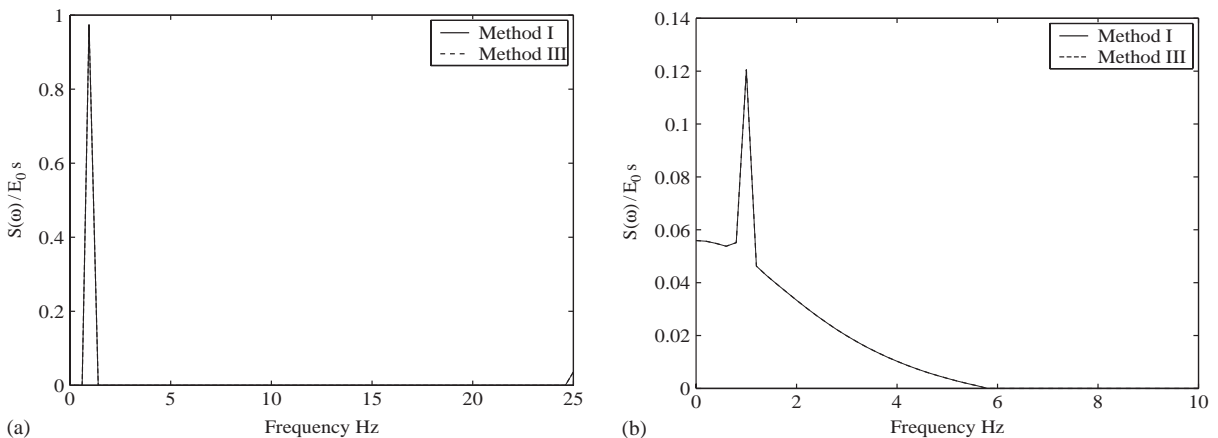


Fig. 4. Example 2: psd of $\ddot{x}_g(t)$. (a) Case 1, (b) case 2; $R = 0.6133 \text{ m}$.

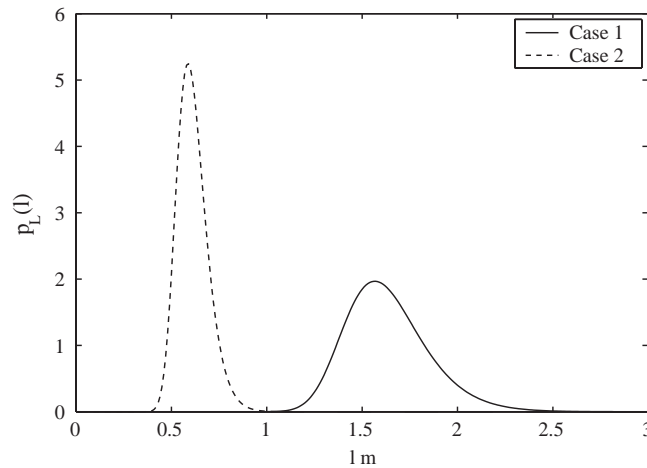


Fig. 5. Example 2: pdf of L_m under critical excitation, method I; $R = 0.6133$ m.

displacement from 0.52 to 0.29 m. The effect of changing the structure resistance R on the estimated failure probability was also studied. The chimney failure probability was computed as 0.0135, 0.0403, 0.1107, 0.2672 and 0.5327 when R was taken as 0.4906, 0.5520, 0.6133, 0.6746 and 0.7360 m, respectively.

6. Conclusions

In this paper, new formulations for deriving critical earthquake excitations for linear structures under random ground motion are developed. These formulations take advantage of the well developed reliability methods, random vibration analysis and nonlinear optimization programming. New definitions for critical inputs in terms of the structure probability of failure and reliability indices are introduced. Specifically three methods have been discussed in this paper. These methods (I, II and III) have different scope, are based on different underlying approximations and, therefore, have different ranges of validity. The application of method I requires the knowledge of probability distribution of extremes of the load effects over a specified duration. When load effects could be modelled as Gaussian random processes, as in the case of response of linear systems to Gaussian excitations, the extreme values can be modelled as Gumbel random variables. Within the framework of this method, treatment of structural uncertainties, nonlinearities, and non-Gaussian load effects (such as, for example, von Mises stress in a linear structure subjected to Gaussian excitations), are difficult to handle. Method II has similar aspirations as method I: here again the objective is to maximize probability of failure, but this is achieved approximately and indirectly. This method is based on the orderability character of the Hasofer–Lind reliability index, that is, any increase in this index signals a reduction in failure probability. Here the performance function is linearized around the check point in the standard normal space. The method is more generally applicable: it can handle uncertainties in structural uncertainties (such as, randomness in mass, stiffness, damping and strength characteristics), their

non-Gaussian nature, and mutual dependencies between loads and structural parameter variations. The application of this method provides, as a byproduct of the analysis, information on sensitivity of critical response to different parameters of the problem. The method essentially introduces concepts from theory of reliability indices into the development of critical excitation modelling: this, we believe, to be a novel application of theory of such indices. Method III works at the level of second-order response moments, and, therefore, has relatively narrower scope: its extension to handle structural uncertainties and nonlinearity is not straightforward.

Thus, it is clear that, it may not be straight forward to solve a given problem using all the three methods. However, for a subset of problems, as has been considered in the present study, all the three methods are indeed applicable. The study of these subset of problems enables one to compare the relative performance of the three methods. Even for these problems, viewed from a mathematical perspective, the details of the objective functions are still different for the three methods and, in this sense, it is hard to anticipate in advance that the three methods should lead to similar results. Specifically, it must be noted that the basic aspirations of methods I and II are similar, that is, to produce critical excitations that maximize the probability of failure. However, as has been already emphasized, method II is relatively more approximate in nature, and more generally applicable than method I. Thus, the observation that the alternative methods, for the performance functions considered in this study, lead to similar critical excitation models points towards acceptability of working of method II. This agreement also provides the necessary confidence to extend the applicability of method II to more general class of problems. In the treatment of seismically loaded nonlinear and/or parametrically excited systems, information on extreme value distribution of response over a given duration is often not available. This impedes the application of method I to this class of problems. On the other hand, with the currently available tools of structural reliability analysis, it is feasible to compute reliability indices associated with nonlinear and/or parametrically excited systems, although, the determination of the probability density function of extreme values for the response of these systems is still difficult. Thus, using methods based on response surface techniques, one can approximately evaluate reliability index, even when no analytical estimates for extreme value distributions are available. Studies on development of critical excitation models for a class of nonlinear systems subject to random earthquake loads is considered in the sequel to the present study [21].

The following are a few limitations of the present study, which, further research efforts can eliminate:

- The extreme value theory used in implementing method I is valid asymptotically and is based on the assumption of stationarity of excitations and Poisson approximation for the number of level crossings. This result can be improved upon by introducing nonstationary amplitude and frequency content model for the seismic excitations and by using more refined theories for modelling extremes.
- The definition of critical excitations in this study is based on a single performance criterion. This definition can usefully be modified to allow for more than one failure modes into the characterization of structural failure. The consequent analysis for critical excitations requires the application of time variant system reliability concepts. Within the framework of method III, critical excitations that simultaneously maximize the response variance associated with a vector of response variables can be handled by using methods of multi-objective optimization.

- Method II is essentially approximate in nature since, the method employs first-order reliability methods that are based upon linearization of performance function about the check point in the standard normal space. Consequently, given the nonlinear nature of the performance function, the knowledge of β is not always guaranteed to lead to an acceptable estimate of the probability of failure. The results could be improved if one employs second-order reliability methods and, also, if one uses refined computational procedures as developed, for example, by Der Kiureghian and Dakessian [23], to take into account possible existence of multiple design points.
- The problems of constrained nonlinear optimization that underlie the study reported in this paper have been solved using sequential quadratic programming tools. Generally, these methods are not guaranteed to give the global optimal solutions. In the present study, this issue has been examined essentially numerically. In fact, it was generally observed that initiating numerical optimization steps with different starting guesses lead to the same optimal solutions. Furthermore, these solutions were considered acceptable since they displayed qualitatively the features that could be explained in a consistent manner. In this context, the use of alternative powerful optimization tools such as those based on genetic algorithms, should be of interest.
- In the present study we have treated the constraints on critical inputs as being deterministic in nature. The long-range uncertainties associated with the earthquake phenomenon can be taken into account by treating these constraints used as being random in nature. In this context, it is of interest to note that Bayesian methods, that are developed in reliability literature to deal with distributional parameter uncertainties, could provide useful framework to develop and update critical excitation models.

Acknowledgements

The work reported in this paper has been partly supported by funds from the Department of Science and Technology, Government of India.

References

- [1] C.S. Manohar, A. Sarkar, Critical earthquake input power spectral density function models for engineering structures, *Earthquake Engineering and Structural Dynamics* 24 (1995) 1549–1566.
- [2] I. Takewaki, Seismic critical excitation method for robust design: a review, *Journal of Structural Engineering* 128 (2002) 665–672.
- [3] R.F. Drenick, Model-free design of aseismic structures, *Journal of Engineering Mechanics* 96 (4) (1970) 483–493.
- [4] M. Shinozuka, Maximum structural response to seismic excitations, *Journal of Engineering Mechanics* 96 (5) (1970) 729–738.
- [5] R.N. Iyengar, Matched inputs, Report 47, Series J, Center of Applied Stochastics, Purdue University, West Lafayette, Ind, 1970.
- [6] R.N. Iyengar, C.S. Manohar, Nonstationary random critical excitations, *Journal of Engineering Mechanics* 133 (4) (1987) 529–541.
- [7] R.N. Iyengar, Critical seismic excitation for structures, *Proceedings of the Fifth ICOSSAR Conference*, vol. 25, San Francisco, 1989, pp. 29–37.

- [8] M. Srinivasan, R. Corotis, B. Ellingwood, Generation of critical stochastic earthquakes, *Earthquake Engineering and Structural Dynamics* 21 (1992) 275–288.
- [9] I. Takewaki, Optimal damper placement for critical excitation, *Probabilistic Engineering Mechanics* 15 (2000) 317–325.
- [10] I. Takewaki, A new method for non-stationary random critical excitation, *Earthquake Engineering and Structural Dynamics* 30 (2001) 519–535.
- [11] S. Khajepour, A. Sarkar, Development of optimally disordered critical random excitation using adaptive computing, *Journal of Sound and Vibration* 244 (5) (2001) 871–881.
- [12] A. Sarkar, S. Khajepour, Response level crossing rate of a linear system excited by a partially specified Gaussian load process, *Probabilistic Engineering Mechanics* 17 (2001) 85–95.
- [13] A.M. Abbas, C.S. Manohar, Investigations into critical earthquake load models within deterministic and probabilistic frameworks, *Earthquake Engineering and Structural Dynamics* 31 (2002) 813–832.
- [14] A. Sarkar, C.S. Manohar, Critical cross power spectral density functions and the highest response of multi-supported structures to multi component earthquake excitations, *Earthquake Engineering and Structural Dynamics* 25 (1996) 303–315.
- [15] A. Sarkar, C.S. Manohar, Critical seismic vector random excitations for multi-supported structures, *Journal of Sound and Vibration* 212 (3) (1998) 525–546.
- [16] A.M. Abbas, C.S. Manohar, Critical spatially varying earthquake load models for extended structures, *Journal of Structural Engineering* 29 (1) (2002) 39–52.
- [17] N.C. Nigam, *Introduction to Random Vibration*, MIT Press, London, 1983.
- [18] M.A. Branch, A. Grace, *Matlab Optimization Toolbox, User's Guide*, The MATH WORKS Inc., 1996.
- [19] A.H.-S. Ang, W.H. Tang, *Probability Concepts in Engineering Planning and Design: Vol. II, Decision, Risk and Reliability*, Wiley, New York, 1984.
- [20] A.M. Hasofer, N. Lind, An exact and invariant first-order reliability format, *Journal of Engineering Mechanics* 100 (1) (1974) 111–121.
- [21] A.M. Abbas, C.S. Manohar, Reliability-based critical earthquake load models. Part 2: nonlinear structures, *Journal of Sound and Vibration* 287 (4 + 5) (2005) 883–900; doi:10.1016/j.jsv.2004.12.003.
- [22] S.W. Crawley, R.M. Dillon, *Steel Buildings: Analysis and Design*, third ed., Wiley, New York, 1984.
- [23] A. Der Kiureghian, T. Dakessian, Multiple design points in first and second-order reliability, *Structural Safety* 20 (1998) 37–49.